Next-generation all-solid-state battery (#ASSB)

Tuan Vo^{a,b†}, Claas Hüter^b, Stefanie Braun^a, Manuel Torrilhon^a

^aDepartment of Mathematics, Applied and Computational Mathematics (ACoM), RWTH Aachen University, Schinkelstraße 02, 52062 Aachen, Germany ^bInstitute of Energy and Climate Research (IEK-2), Forschungszentrum Jülich, Wilhelm-Johnen-Straße, 52428 Jülich, Germany

Mathematical modelling for the next-generation All-solid-state batteries: Nucleation (SE|SSE)^(*)-interface

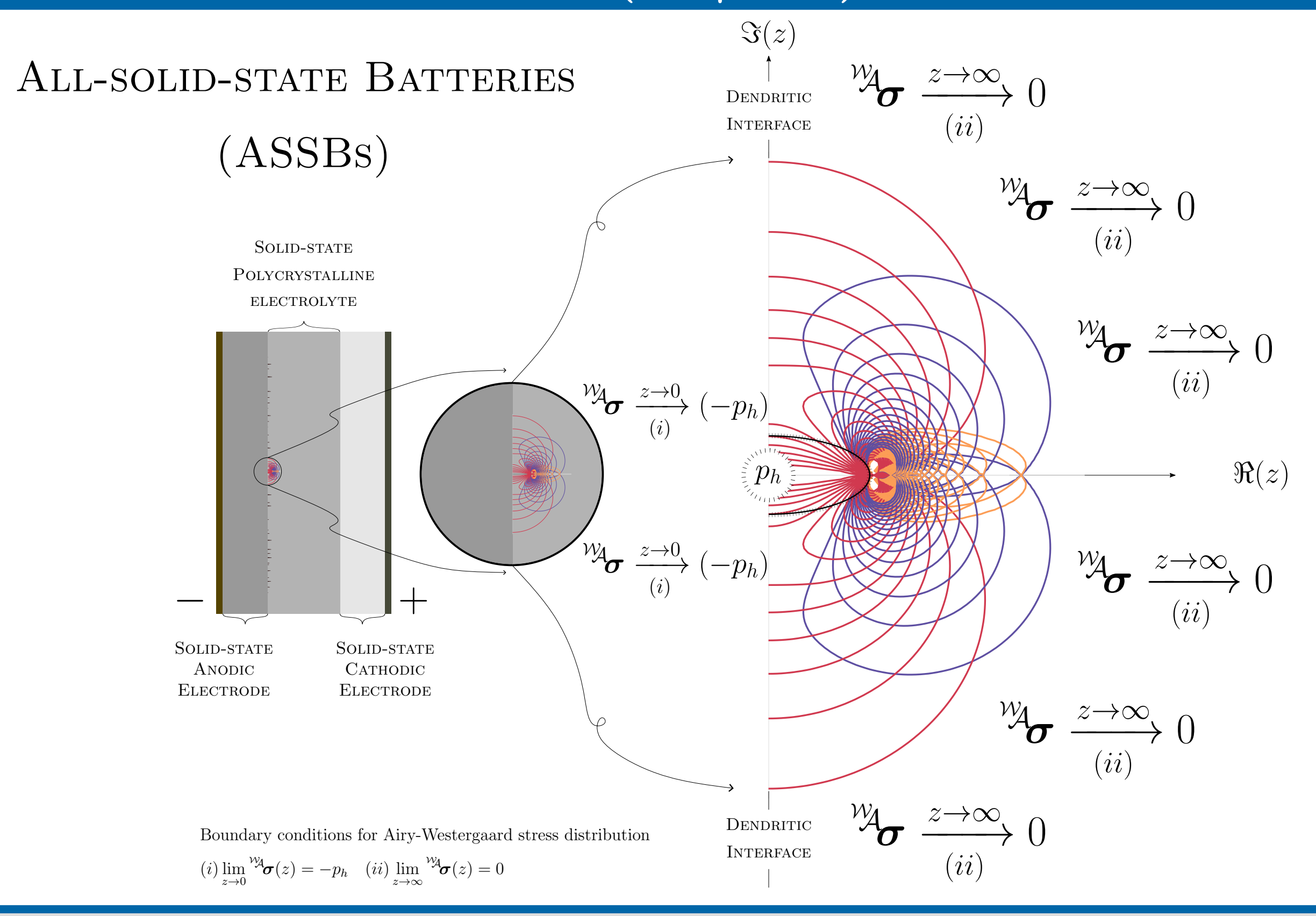
Rechargeable Lithium-ion battery (LIB) is at the heart of every electric vehicle (EV), portable electronic device, and energy storage system [1]. Nowadays, LIBs enable human life more efficient and help to solve global environment issues thanks to EVs' zero emission. However, conventional LIB (c-LIB) is sensible to temperature and pressure, hence, flammable and explosive, which is undesirable. This bottleneck is mainly due to liquid-based electrolyte found in c-LIBs.

All-solid-state battery (ASSB) is one of promising candidates to overcome bottlenecks of c-LIBs. Thanks to solid-state electrolyte (SSE), ASSB is highly stable towards temperature and pressure. Nevertheless, Limetal dendrite triggered at (SE|SSE)-interface [5] is the main drawback of ASSB since these dendritic threads extrapolate into SSE grain boundary network, causing crevice, degradation of ionic conductivity, and the probability of short-circuit, which is unfavorable.

Next-generation All-solid-state battery (ng-ASSB) with a consideration of nucleation criterion defined by

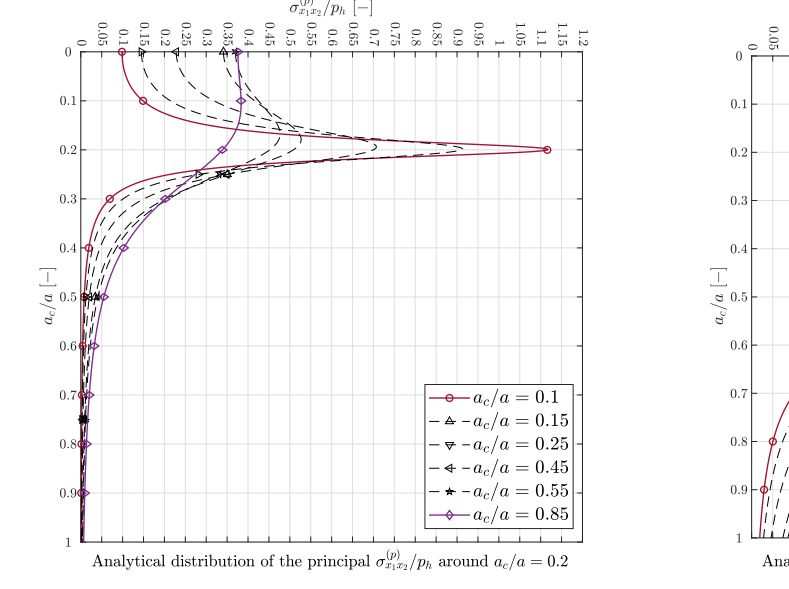
$$a_{\text{Griffith}} := a^* = \arg\min_{a \in \mathbb{R}} \left. \iint_{\Omega} f(a, \boldsymbol{u}, \theta; \lambda, \mu, \boldsymbol{d} \otimes \boldsymbol{d}) \, d\Omega - \left. \iint_{\Gamma} f(a; \gamma) \, d\Gamma \right|_{\boldsymbol{u}} d\beta$$

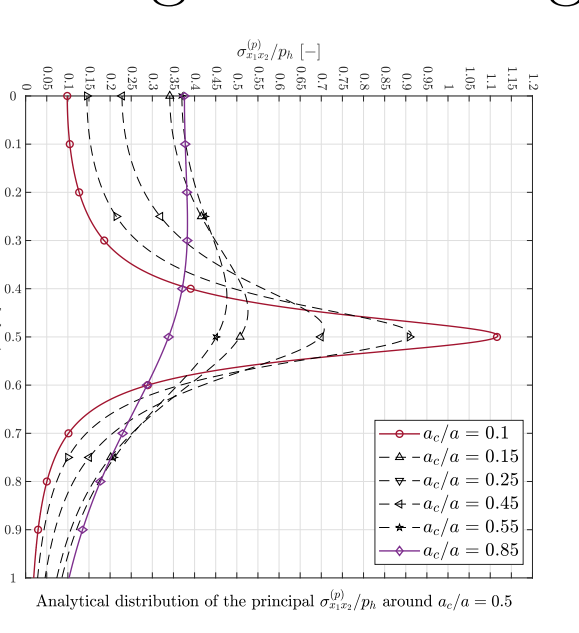
where \boldsymbol{u} displacement field, θ temperature field, a crevice length, λ, μ Lamé constants, $\boldsymbol{d} \otimes \boldsymbol{d}$ embedded misorientation structural tensor, and γ cracking-surface energy density, can help to improve ASSB performance.

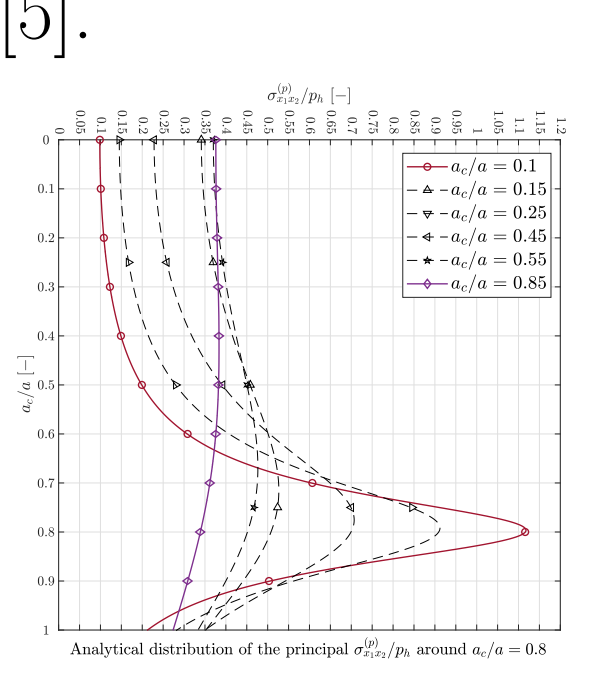


Interface Analysis

Interface between solid electrode and solid-state electrolyte (SE|SSE) taking place at space charge layer (SCL) [2] found in ASSBs critically exhibits mechanical and electrochemical instability [3]. This evidence points directly to the fact that the soft metallic li anode is erroneously prone to triggering dendrites, under cycles of electric charge & discharge [5].



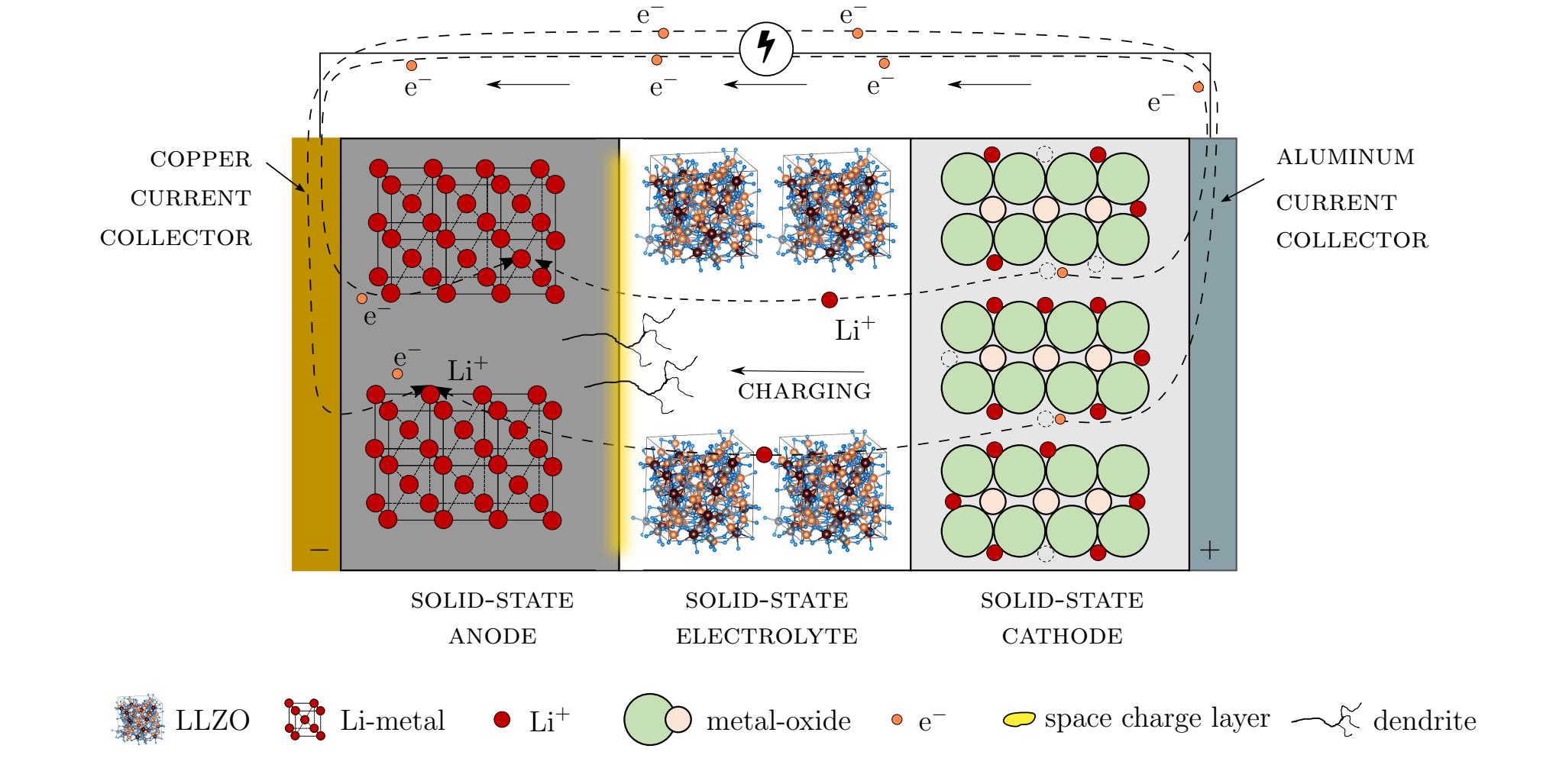




<u>Distribution</u>: ana. max. shear stress ${}^{\mathcal{W}}\!\!\sigma_{x_1x_2}^{\Pi}$ around crack tip a_c .

Next-generation All-solid-state battery

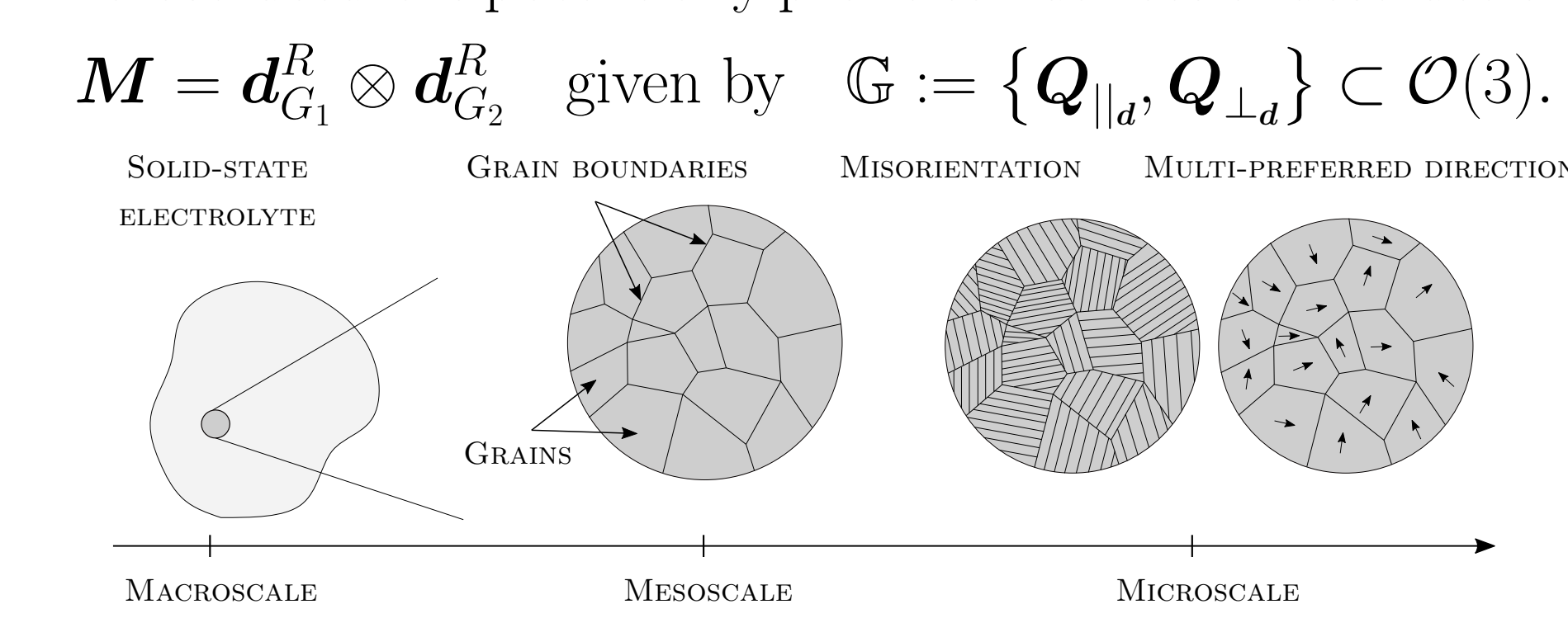
Nucleation criterion governs the instable (SE|SSE)-interface [3]



Thermodynamic consistency is satisfied, followed by [2]. ✓ Closure $\bar{\Omega}$ is fulfilled by 15 moments, followed by [4].

Embedded structural-tensor SSE

Polycrystalline garnet-type SSE [5] such as LLZO exhibit grain boundary network, and grains with variation of {size, shape} under microscopic observation. Hence, this microstructure is potentially prone to nuances of destruction.



Consequentially, dendrites contribute to degradation of ionic conductivity and tiny-cracks tracing along grain boundaries.

Nucleation interface: Taking place at the critical dendritic interface

Coupled fields: Displacement vector field and temperature scalar field

$$\boldsymbol{u}: \begin{cases} \Omega \times \mathbb{R}_{+} \to \mathbb{R}^{3}, \\ (\boldsymbol{x},t) \mapsto \boldsymbol{u}(\boldsymbol{x},t), \end{cases} \quad \theta: \begin{cases} \Omega \times \mathbb{R}_{+} \to \mathbb{R}, \\ (\boldsymbol{x},t) \mapsto \theta(\boldsymbol{x},t), \end{cases} \quad \theta: \begin{cases} \Omega \times \mathbb{R}_{+} \to \mathbb{R}, \\ (\boldsymbol{x},t) \mapsto \theta(\boldsymbol{x},t), \end{cases}$$

Governing conservation equations

$$\frac{d}{dt} \int_{\Omega}^{\infty} (\cdot) \ d\Omega = \int_{\Omega}^{\infty} (\cdot)^{\text{action}} \ d\Omega + \int_{\partial \Omega}^{\infty} (\cdot)^{\text{action}} \ d\partial\Omega + \int_{\Omega}^{\infty} (\cdot)^{\text{production/source/sink}} \ d\Omega$$

 $\rho(\boldsymbol{x},t)$ is mass density per unit volume (puv); $\boldsymbol{b}(\boldsymbol{x},t)$ body force puv; $\boldsymbol{v}(\boldsymbol{x},t)$ velocity; $e(\boldsymbol{x},t)$ internal energy puv; $\boldsymbol{q}(\boldsymbol{x},t)$ heat flux; $r(\boldsymbol{x},t)$ heat source puv; $\boldsymbol{\sigma}$ Cauchy stress and ε infinitesimal strain. Helmholtz energy functional

$$a_{\text{Griffith}} := a^* = \arg\min_{a \in \mathbb{R}} \left. \iint_{\Omega} f(a, \boldsymbol{u}; \lambda, \mu, \boldsymbol{d} \otimes \boldsymbol{d}) \, d\Omega - \left. \iint_{\Gamma} f(a; \gamma) \, d\Gamma \right|_{\boldsymbol{u}^{(s)}}$$

Governing PDE

$$a_{\text{Grifflith}} := a^* = \arg\min_{a \in \mathbb{R}} \left. \iint_{\Omega} f(a, \boldsymbol{u}; \lambda, \mu, \boldsymbol{d} \otimes \boldsymbol{d}) \, d\Omega - \left. \iint_{\Gamma} f(a; \gamma) \, d\Gamma \right|_{\boldsymbol{u}^{(s)}}$$

abc

Strain energy: Interface between solid electrode and solid-state electrolyte (SE|SSE) taking place at space charge

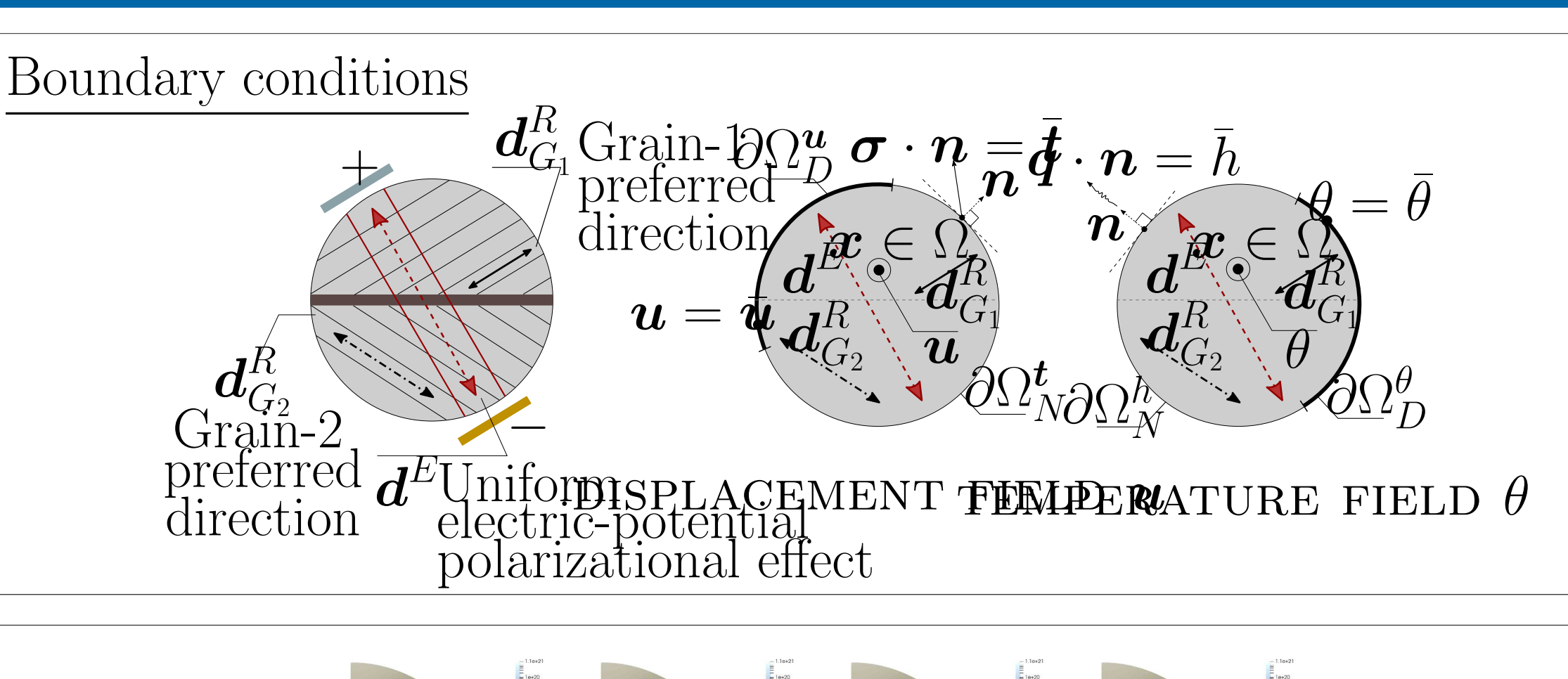
 $\iiint_{\Omega} f(a, \boldsymbol{u}; \lambda, \mu, \boldsymbol{d} \otimes \boldsymbol{d}) d\Omega$

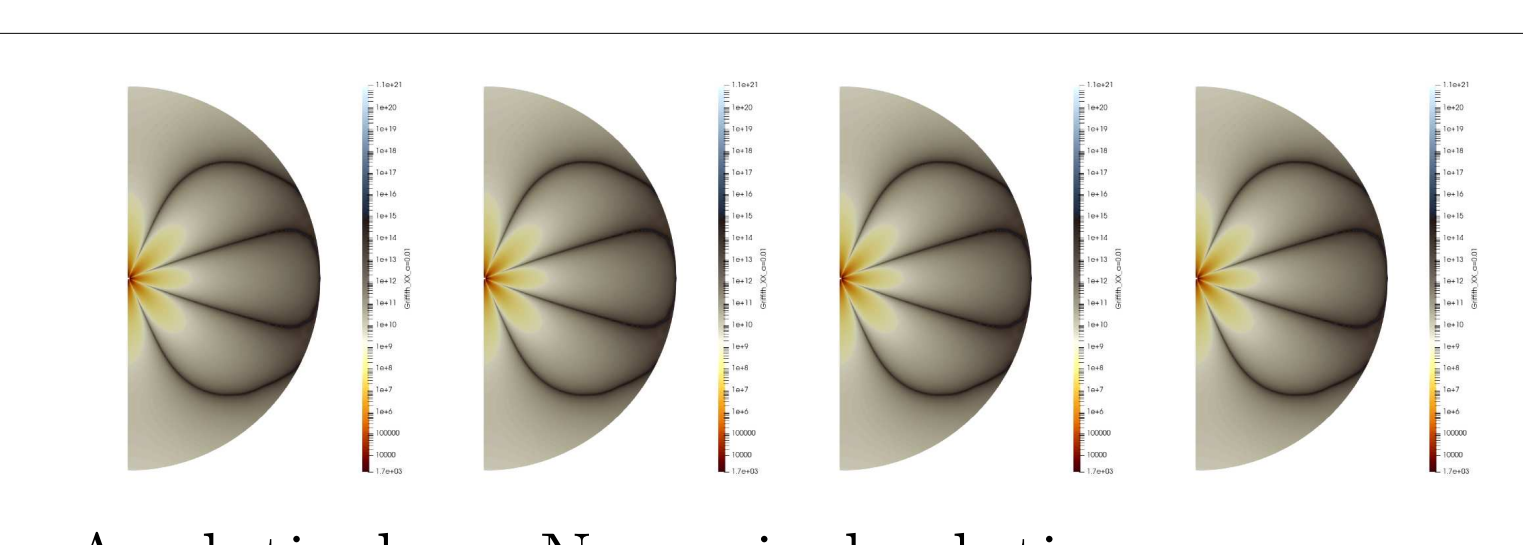
Surface energy: Interface between solid electrode and solid-state electrolyte (SE|SSE) taking place

$$\iint_{\Gamma} f(a; \gamma) \, d\Gamma$$

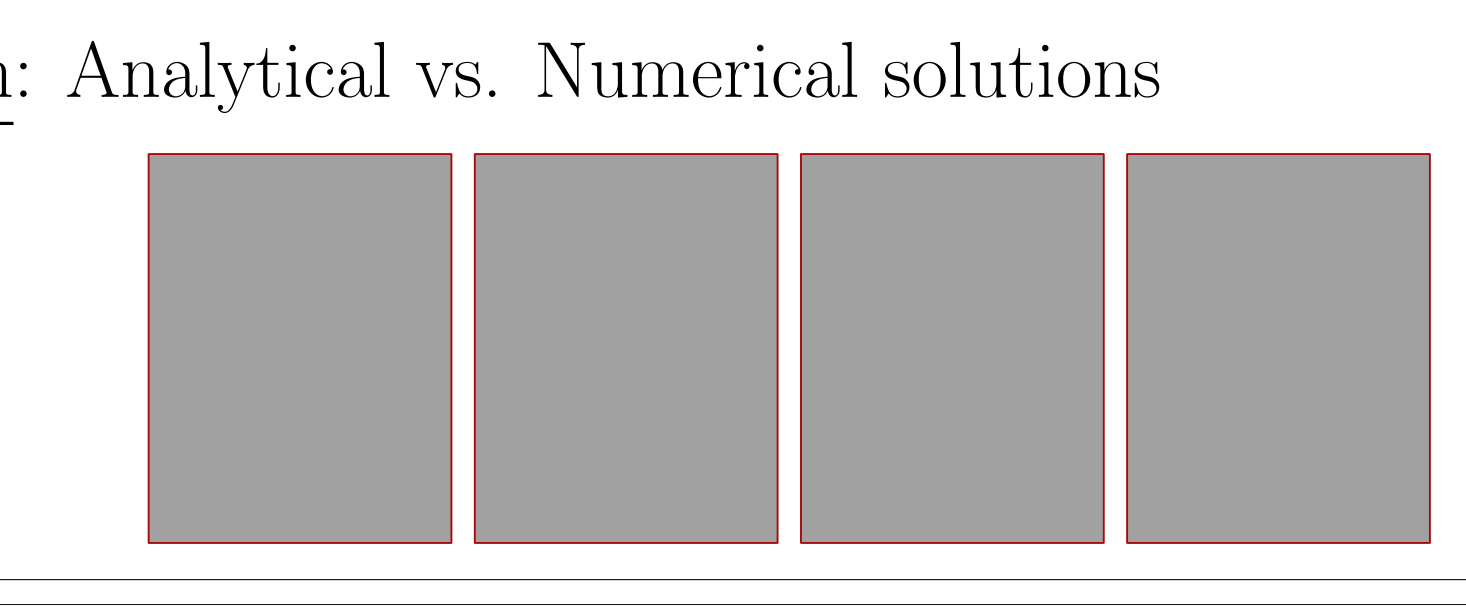
Therefore

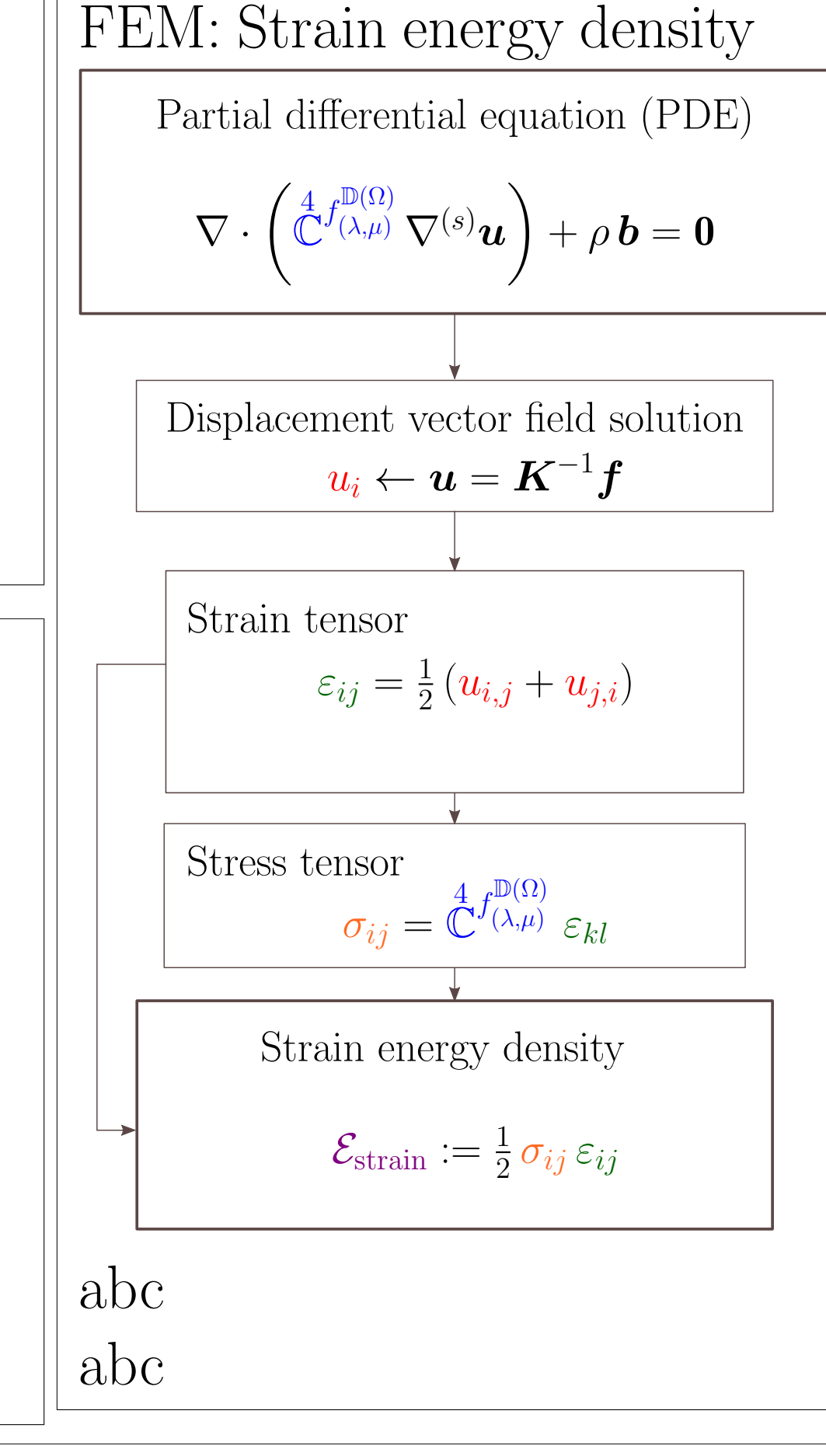
$$\rho \, \partial_{t^2}^2 \boldsymbol{u}^{(s)} + \nabla \cdot \left(\stackrel{4}{\mathbb{C}} f_{(\lambda,\mu)}^{\mathbb{D}(\Omega)} : \nabla \boldsymbol{u}^{(s)} \right) + \rho \nabla V_e = \mathbf{0},$$
s.t. $a_{\text{Griffith}} := a^* = \arg\min_{a \in \mathbb{R}} \left. \iint_{\Omega} f(a, \boldsymbol{u}; \lambda, \mu, \boldsymbol{d} \otimes \boldsymbol{d}) \, d\Omega - \int_{\Gamma} f(a; \gamma) \, d\Gamma \right|_{\boldsymbol{u}^{(s)}}$
abc





Comparison: Analytical vs. Numerical solutions





Airy-Westergaard function used for stress analysis: (i) max. shear stress and (ii) principal stresses

$$\mathcal{W}_{\mathcal{A}}: \begin{cases} \mathbb{C} \to \mathbb{C}, \\ z \mapsto \mathcal{W}_{\mathcal{A}}(z) := \Re(\iint_{\Gamma} \mathcal{K}^{(\star)} \, dz) + x_2 \Im(\oint_{\Gamma} \mathcal{K}^{(\star)} \, dz), \end{cases} \quad \mathcal{K}^{(\star)}: \begin{cases} \mathbb{C} \to \mathbb{C}, \\ z \mapsto \mathcal{K}^{(\star)} := -p_h + p_h/\sqrt{1 - a^2/z^2}, \end{cases}$$

where a the crevice length, p_h pressure at the opening crevice on dendritic interface, and $\forall \{p_h, a\} \in \mathbb{R}_+$.

FEM implementation: element matrix \mathbf{K}^e approx. by Gauss quadrature; indices imply 4+2=6 for-loop: $K_{ik}^{e^{\alpha\beta}} = \int_{\Omega^{\xi}} \left(\mathcal{L}_{1}^{\alpha} \, \mathbb{C}_{i1k1}^{fGL}(y) \, \mathcal{R}_{1}^{\beta} + \mathcal{L}_{1}^{\alpha} \, \mathbb{C}_{i1k2}^{fGL}(y) \, \mathcal{R}_{2}^{\beta} + \mathcal{L}_{2}^{\alpha} \, \mathbb{C}_{i2k1}^{fGL}(y) \, \mathcal{R}_{1}^{\beta} + \mathcal{L}_{2}^{\alpha} \, \mathbb{C}_{i2k2}^{fGL}(y) \, \mathcal{R}_{2}^{\beta} \right) \det(\boldsymbol{J}) \, d\Omega^{\xi}$

where \mathcal{L}_{i}^{α} and \mathcal{R}_{l}^{β} are gradients of basis functions at node α^{th} and β^{th} , respectively.

Contact

Tuan Vo vo@acom.rwth-aachen.de



References

[1] **T.Vo**, Modeling the swelling phenomena of li-ion batt. cells based on a numerical chemo-mech. coupled approach. MA, Robert Bosch Battery Systems GmbH, **2018**.

- [2] **S.Braun**, C. Yada and A. Latz, *Thermodynamically consistent model for Space-Charge-Layer formation in a solid electrolyte*. Jr. Phys. Chem., 119, 22281-22288, **2015**.
- [3] **C.Hüter**, S.Fu, M.Finsterbusch, E.Figgemeier, L.Wells, and R.Spatschek, *Electrode-electrolyte interface stability in solid state electrolyte system: influence of* coating thickness under varying residual stresses. AIMS Materials Science, 4(4):867-877, **2017**.
- [4] **M.Torrilhon**. Modeling nonequilibrium gas flow based on moment equations. Annual Review of Fluid Mechanics, 48(1):429-458, **2016**.
- [5] **S.Kim**, J.S.Kim, L.Miara, Y.Wang, S.K.Jung, S.Y.Park, Z.Song, H.King, M.Badding, J.M.Chang, V.Roev, G.Yoon, R.Kim, J.H.Kim, K.Yoon, D.Im, and K.Kang, High-energy and durable li metal batt. using garnet-type solid electrolytes with tailored li-metal compatibility. Nature Communications, 13(1):1883, 2022.









